Far and mid-infrared studies of star forming regions

Koumpia, Evgenia

Chapter 1

Introduction

Understanding the physics and chemistry that take place in regions forming both low and high mass stars, especially the earliest, highly embedded evolutionary stages of star formation is the general topic of this thesis. Star forming regions are among the most chemically rich and complex regions of the Universe and they are located in dense parts of the interstellar medium. The study of their molecular content is one of the major goals of astrochemistry in general and this thesis in particular. But why are we so interested in the chemical composition of these regions?

We know that several processes during star formation influence the chemical composition, complexity and evolution of the interstellar medium. Additionally, the chemical composition and evolution of the interstellar medium have their own influence on the evolution and possibly the mass of a newly born star. The dynamical processes that lead to the collapse of an interstellar cloud and thus the creation of a protostar are highly connected with the chemical composition of the gas. The thermal pressure of the gas and the magnetic fields resist the gravitational forces and thus the collapse, and both are connected with the chemical composition of the medium. Namely, the thermal balance can only be understood if we know: what kind of molecules can be formed, when and where do they form and how much do they contribute on the cooling of the gas via line emission? What are the main heating mechanisms during star formation? The magnetic fields on the other hand, are coupled with the medium through ions. Knowing the ionization structure and the abundance of ions is mandatory to understand the overall star formation processes.

Another topic of interest is understanding the evolutionary stages of very young objects. The processes that turn a prestellar core to a protostar and the several evolutionary stages can be probed by molecular and dust emission. Molecular emission is a powerful tool in probing the several mechanisms that take place during star formation since different chemical species probe different regions and conditions (i.e. temperature, density, velocity distribution). A question of observational importance is: what are the main observational signatures that one can use in order to distinguish the different evolutionary stages?

Last, but not least, understanding the formation/destruction of molecules in star formation is directly connected with understanding the chemical history of stars and planetary systems. Complex organic molecules, which are the building blocks of life, have been observed towards young protostars. How, where and in which form do they form? Studying and understanding the chemical reactions and evolution in star forming regions

could eventually lead to understanding their distribution in protoplanetary systems and to get closer to maybe understand how prebiotic molecules form and the origin of life on Earth.

The purpose of this chapter is to describe the scientific context of this thesis and to give an overview of its commonly used terms, followed by an outline of the observational data and the methods used in our attempt to approach the topics mentioned above. At the end of this chapter the reader finds the specific questions that this thesis addresses and a summary of the scientific chapters that aim to provide answers to these questions.

1.1 Interstellar Medium

The Interstellar Medium (ISM) plays an essential role when it comes to the study of Star Formation, which is the broader topic of this thesis. Stars form within the densest regions of the ISM, while the presence of complex molecules in these regions could be (in)directly connected to the origin of life itself, which may develop on planets around stars.

The ISM fills the space between the stars in galaxies, and it is a combination of dust ($\sim$ 1 % by mass) and gas ($\sim$ 99 %) in ionic, atomic and molecular form. The average density of the ISM is $10^0 - 10^1$ cm^{-3}, but its distribution is highly inhomogeneous. In cool, dense regions of the ISM, matter is primarily in molecular form, and reaches number densities of $>10^6$ molecules cm^{-3}. In hot, diffuse regions of the ISM, matter is primarily ionized, and the density may be as low as 10^{-4} ions cm^{-3}.

The ISM can be cool ($10 - 100$ K), warm ($10^3 - 10^4$ K) and hot ($10^4 - 10^6$ K) and it is spread throughout the host galaxies with the cooler parts in dense interstellar clouds. Depending on the density and temperature of a given cloud, the hydrogen in it can be neutral (HI regions), ionized (HII regions), or molecular. Interstellar clouds are divided into dense clouds ($A_V > 2$ mag, $n_H > 10^4$cm^{-3}) and diffuse clouds ($A_V \sim 0.3 - 2$ mag, $n_H \sim 100 - 500$ cm^{-3}). The classification and transition from a diffuse atomic to a dense molecular cloud can be seen in Figure 1.1.

From the various forms of ISM that were briefly introduced above, we will focus on Molecular Clouds since they provide the host environment for Star Formation. For more background about the ISM and atomic/molecular clouds, see the book from "Physics of the Interstellar and Intergalactic Medium" (Draine 2011) and the review "Diffuse Atomic and Molecular Clouds" (Snow & McCall 2006).

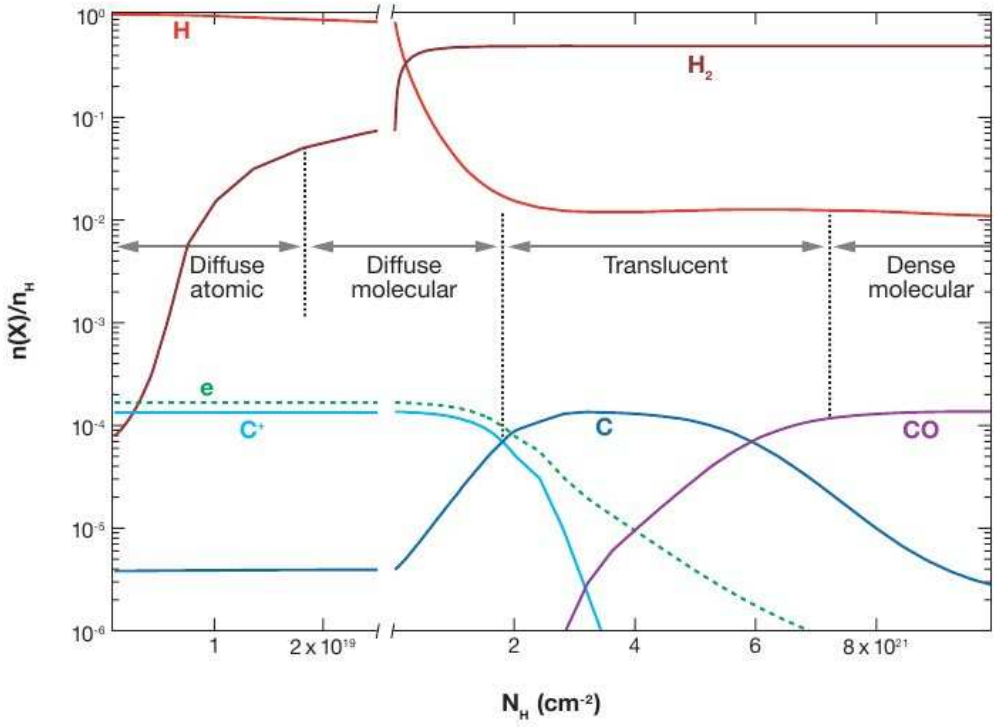

Figure 1.1: Definitions of cloud types (Snow & McCall 2006).

1.1.1 Molecular Clouds

It was $\sim$ 1970 when astronomers first realized that dense interstellar clouds do not actually mainly consist of atoms but molecules as well (Dieter & Goss 1966). This is a crucial difference since molecular clouds are denser and cooler than the atomic clouds and those properties are exactly what make them ideal sites for the formation of stars. The density and size of these objects permits the formation of molecules, with the molecular hydrogen (H_2) the most common, followed by some heavier species. Cold H_2 is difficult to observe by infrared observations (Tielens 2005) for two reasons: it is symmetric and thus the pure rotational lines are dipole–forbidden, providing only weak quadrapole transitions, and it has low mass, which means that the energy levels are high, so that the lines appear in the mid–IR and they trace warmer gas. The ro-vibrational lines appear in near–IR and they trace mainly hot gas ($\sim$1000 K, e.g. shocks).

The next abundant molecule often used in this thesis, CO, has a small but nonzero dipole moment, and is therefore widely used as a tracer of cold H_2 in dense molecular clouds because it has an almost constant, stable and high abundance (H_2/CO $\sim$ 10^4; Tielens 2005). The formation of molecules depends on extinction and somewhat on the density. Figure 1.1 shows exactly this dependence: we can see that H_2 begins to form

in diffuse molecular clouds ($A_V \sim 0.5$), while CO begins to form in translucent clouds ($A_V \sim 1.2$), with the exact boundary depending on the radiation field. Using Herschel, Langer et al. (2010) present ~30 H_2 diffuse clouds ($A_V < 1.3$) that interestingly, show [CII] and HI emission but no associated CO emission. This finding was the first observed evidence for the presence of warm molecular "dark gas" (hidden layer of H_2) in diffuse regions. Grenier et al. (2005) also unveiled clouds of cold dust and dark gas, invisible in HI and CO but detected in γ rays.

Observations in other galaxies show that the conversion factor between the observed CO intensity I(CO) and the H_2 column density N(H_2) as measured is not universal, but changes with metallicity, cosmic ray density and UV radiation field. The observed "X-factor" X = N(H_2)/I(CO) is of order 10^{20} mol cm^{-2}/K km s^{-1} for giant spirals and rises up to the order of 10^{21} mol cm^{-2}/K km s^{-1} for dwarf irregulars (Boselli et al. 2002). In the Milky Way disk, which is more relevant to the galactic sources studied in this thesis, the "X-factor" is 2×10^{20} mol cm^{-2}/K km s^{-1} (Bolatto et al. 2013).

Molecular clouds are often inhomogeneous, showing structure of clumpiness, consisting of several denser regions ($10^2 - 10^4$ cm^{-3}). Signposts of (massive) star formation include infrared sources, HII regions and masers. There is evidence that inside these regions the formation of massive stars is also taking place (Zinnecker & Yorke 2007; Beuther et al. 2007). The main mechanisms that are responsible for those inhomogeneities in molecular clouds are turbulence, magnetic fields, shock waves and stellar winds, leading to the formation of clumpy structures that lead to star formation.

A big part of this thesis focuses on the study of the interaction between the radiation that the newly born stars emit and their surrounding ISM. The best environments to study the influence of the far ultraviolet photons (FUV) from stars to the ISM are the so called photon dominated regions, also known as photodissociation regions (PDRs).

1.1.2 Photon Dominated Regions – PDRs

PDRs are regions where far ultraviolet photons (FUV) with energies 6 eV $< h\nu <$ 13.6 eV control the thermal balance and chemistry. Classic PDRs are associated with conditions that allow the co-existence of neutral hydrogen, photodissociated molecules and ionized species, such as carbon (C) (ionization potential $<$ 13.6 eV). These conditions can be found in the interface between [HII] regions and molecular clouds. Nowadays, we use the term PDRs for a broader range of regions, including regions where molecular hydrogen is abundant and carbon mostly in CO, such as the surfaces of molecular clouds. These are regions where FUV photons drive the chemistry of oxygen and carbon.

Figure 1.2 presents the structure of a PDR as discussed by Hollenbach et al. (2009). FUV photons from hot stars or the interstellar radiation field penetrate the molecular cloud, resulting in ionization, dissociation and an increasing of gas temperature. The UV radiation field decreases with distance into the cloud, which can be quantified by the

visual extinction A_V. In the [HII] region the field is strong enough to maintain hydrogen in ionized form (HII). The rest of the H–ionizing photons are absorbed in the so called ionization front, which is a thin layer in which the ionization fraction of hydrogen transits from almost fully ionized to almost fully neutral. Hydrogen remains atomic until the attenuation of the H_2 dissociating photons by the dust and the self–shielding of H_2 (in dense PDRs $A_V \simeq 2$). In a similar way carbon (C, $A_V \simeq 2$–4) transits from ionized to neutral which leads to the formation of CO. The location of the CII/C/CO transition depends on the incident radiation field.

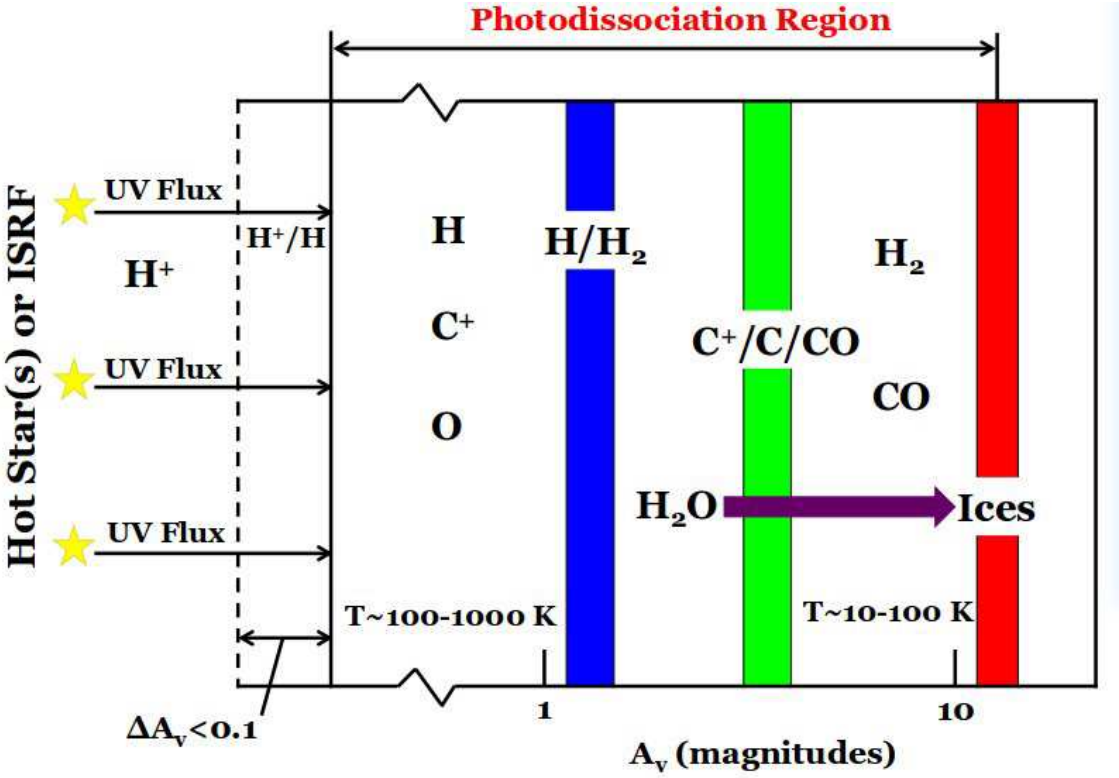

Figure 1.2: Schematic diagram of a PDR showing the structure on the interface of a molecular cloud and an [HII] region, illuminated from the left and up to about $A_V \sim 10$, where O_2 is not photodissociated. The water surface formation and the ices influence the PDR structure at high A_V (Hollenbach et al. 2009). Illustration: M. Kaufman

The structure of PDRs depends basically on two factors: the strength of the radiation field and the density. Densities range from n$\sim$0.25 cm^{-3} in the warm neutral medium (WNM), to n $\sim$10–100 cm^{-3} in diffuse clouds and up to n$\sim 10^3$–10^7 cm^{-3} in PDRs associated with molecular clouds. FUV photons influence the chemistry and ionization balance of the species mentioned above for $A_V < 8$, where most of the mass in molecular clouds lies. Ionized carbon can trace all the phases of ISM mentioned above. Pineda et al. (2013) studied the global distribution of ISM gas components in the galactic plane using the [CII] emission with Herschel and found that most of the observed emission

comes from dense PDRs (∼47%), followed by CO-dark H_2 gas (∼28%), cold atomic gas (∼21%), and a smaller fraction by ionized gas (∼4%). Thus, we can say that most of the ISM is actually in PDRs, a fact that makes their study and understanding very important.

A significant part of this thesis is the study of the thermal balance in the S 140 PDR region and the influence of a clumpy structure on its thermal balance. S 140 is located at the surface of the L 1204 molecular cloud at a distance of 764 pc. There is on–going star–formation in the cloud, as it harbors a cluster of massive young stellar objects. The main heating and cooling mechanisms that take place in such regions and the importance of clumpiness are described below.

1.1.3 Heating and cooling mechanisms in PDRs

The heating of PDRs is mainly the result of two main mechanisms which are both connected to the impact of the FUV: the photoelectric effect on large PAH (polycyclic aromatic hydrocarbon) molecules and small grains and FUV pumping of the H_2 molecules. The dust is mainly heated by the direct absorption of the FUV photons. During the photoelectric heating, the electrons that are injected into the gas phase are characterized by some excess kinetic energy, which results in heating of the gas. The second mechanism is a result of vibrationally excited H_2 in the ground electronic state, that can release its excess vibrational energy by emitting a near–IR photon or by de-excitation through collisions, which also heat the gas. Additional heating processes include the collisional de–excitation by atomic H at high densities ($n > 10^4$ cm^{-3}), cosmic ray heating, the formation of H_2 into an excited state and its dissociation, turbulence and shocks from protostellar outflows and collisions between grains and gas at higher dust temperatures. Gas–grain collisions can also contribute to the general heating of the gas as soon as a gas molecule (usually H_2) collides with a warmer grain, which can cause the increase of its original kinetic energy. This mechanism can become important in the deeper, opaque regions of the PDR (A_v∼5) where the radiation of the embedded stars warms the dust to temperatures that can exceed the gas temperature (Kwok 2007).

On the other hand, in order to understand the thermal balance in PDRs, one has to take into account the cooling processes that take place. The major process that leads to the cooling of the gas is the collisional excitation of far–infrared fine structure lines followed by the emission of a photon. The more important atomic lines during this process are: [CII] at 158 μm, [CI] at 609 and 370 μm, [OI] at 63 μm and 145 μm. Only at larger depths (higher A_V) of the PDR, the ro–vibrational transitions of H_2 and the rotational lines of CO become also important. Lastly, far–infrared continuum emission provides the main cooling of the dust. Gas–grain collisions can also contribute to the general cooling of the gas as soon as dust temperature is lower than the gas temperature and the cooling becomes significant when $T < 50$ K.

1.1.4 PDRs and clumpiness

When one aims to study the properties of a PDR, as we do in this thesis, one needs to understand the factors that allow or block the transfer of FUV radiation in the ISM. Dust absorption and scattering and the geometry of the cloud define to what degree the FUV radiation will penetrate the cloud, which in turn defines the several chemical zones that characterize the PDR. During modeling of such regions the assumption of a homogeneous medium is widely adopted, while the measured properties of the clouds are basically average values and based on specific lines.

It is broadly accepted that the interstellar clouds are not generally homogeneous but they rather show clumpiness, which influences the degree of the FUV penetration into the cloud. In a clumpy environment, the FUV photons can travel deeper in the cloud than in a homogeneous medium. They can penetrate the less dense interclump medium and as a result PDRs are formed on the surfaces of the embedded clumps that face the UV source (Figure 1.3). The penetration of FUV radiation can vary by orders of magnitude for different assumed clump filling factors and density contrast between clump and interclump gas (e.g. Orion Bar; Young Owl et al. 2000; Lis & Schilke 2003). As we described above the FUV radiation is the main heating mechanism of PDRs and thus the clumpy structure of these regions, is a crucial factor in understanding their thermal balance and their chemistry, which is among the main goals of the present thesis.

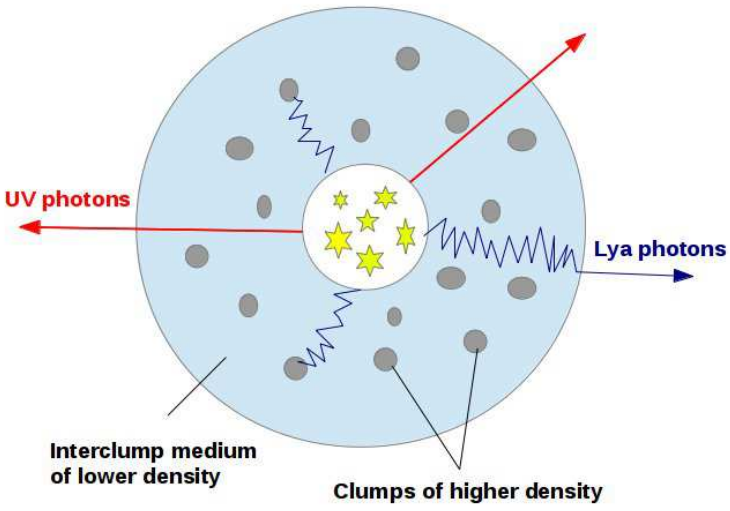

Figure 1.3: Schematic diagram of UV propagation in spherical PDR which is characterized by high density clumps and lower density interclump medium.

1.2 Star Formation

The second goal of this thesis is the understanding of the processes that lead to the formation of the protostar and its evolutionary stages. This section aims to describe the main processes that support or halt the parent cloud from collapsing and create the conditions that favor the protostellar formation.

A cloud of gas will remain in hydrostatic equilibrium as long as its gravitational force is in balance with the gas pressure. A cloud, or a part of it, can leave the equilibrium state and start to collapse, when the gas pressure is not strong enough to balance the gravitational force. The upper limit of the mass of a cloud that is required in order to be in equilibrium, for a given temperature and radius and assuming a spherical symmetry, is known as the Jeans mass M_J and it is described for instance in Stahler & Palla (2005). Once this critical mass is exceeded, the contraction of the cloud will begin until the conditions change in a way that will not allow further collapse. When the central H_2 core is heated up to a point that a hydrostatic balance is achieved, we have the formation of the First Hydrostatic Core (FHSC), which is prior to the real protostar. At that point the temperature of this core increases while the gas keeps falling towards it leading to an additional heating of the core. At about 2000 K the H_2 molecules begin to dissociate, followed by the ionization of hydrogen and helium. These processes allow a second collapse on timescales similar to free fall. When this accretion phase is complete and the internal forces are enough to support the object from further gravitational collapse, we have the formation of the real protostar.

Cooling through molecules, such as CO emission (Tielens 2005), play a crucial role in this process, since their radiation through collisional excitations causes the cooling of the clumps, which leads to further contraction and a fragmentation that favors star birth. Although H_2 is the most abundant molecule in dark clouds it does not provide the basic cooling mechanism, but CO does. Collisions with H atoms and H_2 can raise CO to excited vibrational levels and it will return to its ground vibrational state emitting the energy as radiation. This will cause the cooling of the gas. But this mechanism (vibrational transitions) is efficient at high temperatures (several thousands of Kelvins) and not in lower gas temperatures that characterize the cool environments giving birth to stars. On the other hand, other molecules provide efficient cooling mechanisms at low temperatures, since their lowest excited rotational level is at much lower energy that that of H_2. Cooling is mostly provided by the emission lines of [CII] and [OI]. There are, however, molecular lines such as CO (rotational), OH and H_2O which can become prominent coolants in dense, embedded regions further down to $\sim$10–30 K. H_2O for example is prominent in shock–heated clouds, where sputtering of ice by high–velocity particles becomes important at velocities higher than 10-15 km s^{-1} (van Dishoeck et al. 2013).

Further collapse increases the density of the clumps much more, making them opaque and rather inefficient in releasing the energy through radiation, raising the temperature

which does not permit additional fragmentation. Now the environment has the ideal conditions in order to produce newly born stars. Of course the mechanism as described above is quite simplified since other physical processes also take place inside the clouds, such as rotation, magnetic fields and turbulence, which affect both the collapse and the fragmentation of a cloud. More precisely, turbulence and magnetic fields have been suggested to be the prominent mechanism that prevent clouds from collapsing (Troland & Crutcher 2008; Padoan & Nordlund 2011). A collapsing rotating cloud eventually flattens (conservation of energy and angular momentum), leading to the formation of what we call an "accretion disk". Through accretion the matter from the surroundings is falling into the central part of the structure, known as central protostar.

1.2.1 High and low mass star formation

Although we are aware of the fact that stars of different masses form inside dark clouds, we actually poorly understand the mechanism that leads to formation of high-mass stars (> 8 $M_\odot$). Our understanding of low mass star (< 2 $M_\odot$) formation though, is better. In terms of chemistry, during the cold and dense pre-collapse phase, molecules on the grain surfaces form ices (H_2O, CO, CO_2) and are enriched with more complex molecules. While collapsing, the radiation that comes from the central protostar heats the inner parts of the envelope that surrounds it, and causes the injection of the molecules, that used to form ices, into the gas phase, which triggers further chemical reactions, and therefore the creation of even more complex molecules may occur creating the so called, "hot corinos", that we describe in more detail in Sec. 1.2.3. These phases of star formation are characterized by bipolar outflows, the interaction of which with the surrounding matter causes shocks that compress and heat this matter enriching even more the chemistry of these regions (Bachiller & Pérez Gutiérrez 1997; Tafalla et al. 2000).

On the other hand the theory that describes high-mass star formation is more "open" since there are more gaps in our understanding of the chemical and dynamical processes. The radiation emitted by massive stars is likely to be strong enough to prevent the surrounding material from falling into the pre-stellar core if the accretion is spherical (e.g.; Krumholz & Matzner 2009), so if massive stars form via core accretion like low–mass stars, the accretion must be non-spherical. Theory cannot fully predict the existence of stars more massive than a few tens of solar masses (Zinnecker & Yorke 2007) although observations have revealed even more massive stars (> 150 $M_\odot$; Crowther et al. 2010). Furthermore there is evidence that at least some massive protostars are indeed surrounded by accretion disks (Tan et al. 2014), which leads to the assumption that massive stars may be able to form by a mechanism similar to that of low mass stars. There are additional theories that try to explain high-mass star formation via merging of less massive protostars (Bally & Zinnecker 2005; Yorke & Bodenheimer 2008). Besides the progress of the past decade we still have troubles to fully understand high mass star formation. Both core and competitive accretion theories still face challenges in explaining several important

aspects. On one hand core accretion is challenged when it comes to the fragmentation properties of magnetized/turbulent gas, and the accretion disks and outflows from collapsing cores. On the other hand competitive accretion has toubles to take into account a realistic feedback from MHD outflows while the observed massive starless cores cause an extra challenge for this theory. For a recent review on the topic see Tan et al. (2014).

The present thesis focuses on the first stages of low mass star formation, when the new born star is embedded in and hidden by its surrounding envelope, and the influence that high mass stars have on their nearby ISM (PDRs).

1.2.2 Protostellar evolution

Low mass protostellar evolution is another topic of interest in this thesis. To put this topic in context, we give here a description of the processes that turn a prestellar core into a protostar and the several protostellar stages that are commonly distinguished. From a cloud of gas that begins to collapse until the formation of a star that enters the main sequence, there are several evolutionary stages that are characterized by different properties, lifespans, sizes. Figure 1.4 presents a schematic drawing of the different stages of high and low mass star formation from a prestellar core to the Class III pre–main sequence object.

Low mass phases

The protostellar evolution in low–mass star formation, following the formation of the protostar is becoming reasonably well characterized, but the evolution from a prestellar core to a protostar is not well known. The first hydrostatic core (FHSC) has been suggested to be the missing link between the two stages for few decades already (Larson 1969), but the scarcity of observations makes its characterization and detailed study very difficult. Recent studies have reported only few candidates (e.g. Enoch et al. 2010; Chen et al. 2010; Pineda et al. 2011).

Before attempting to classify any protostellar object it is crucial to have evidence that this object is a protostar in the first place and not a prestellar core. A compact radio/centimeter continuum source accompanied with molecular outflows (i.e. CO), and/or evidence of an internal heating source (e.g. near/mid infrared emission) are signatures that can rule out the prestellar core. The most common way to classify the individual young stellar objects (YSOs) is the shape of their spectral energy distribution (SED). This classification can be seen in Figure 1.5. The classes are considered to be associated with the specific evolutionary stages as described above, and many times the two terms are used to describe the same thing. This is not totally correct since the evolutionary stages represent the theoretical models, while the class is connected to the observed shape of the SED combined with the determined spectral index or the bolometric temperature as determined by the SED, which depends on more parameters such as geometry

and inclination of the source (Robitaille et al. 2007; Launhardt et al. 2013).

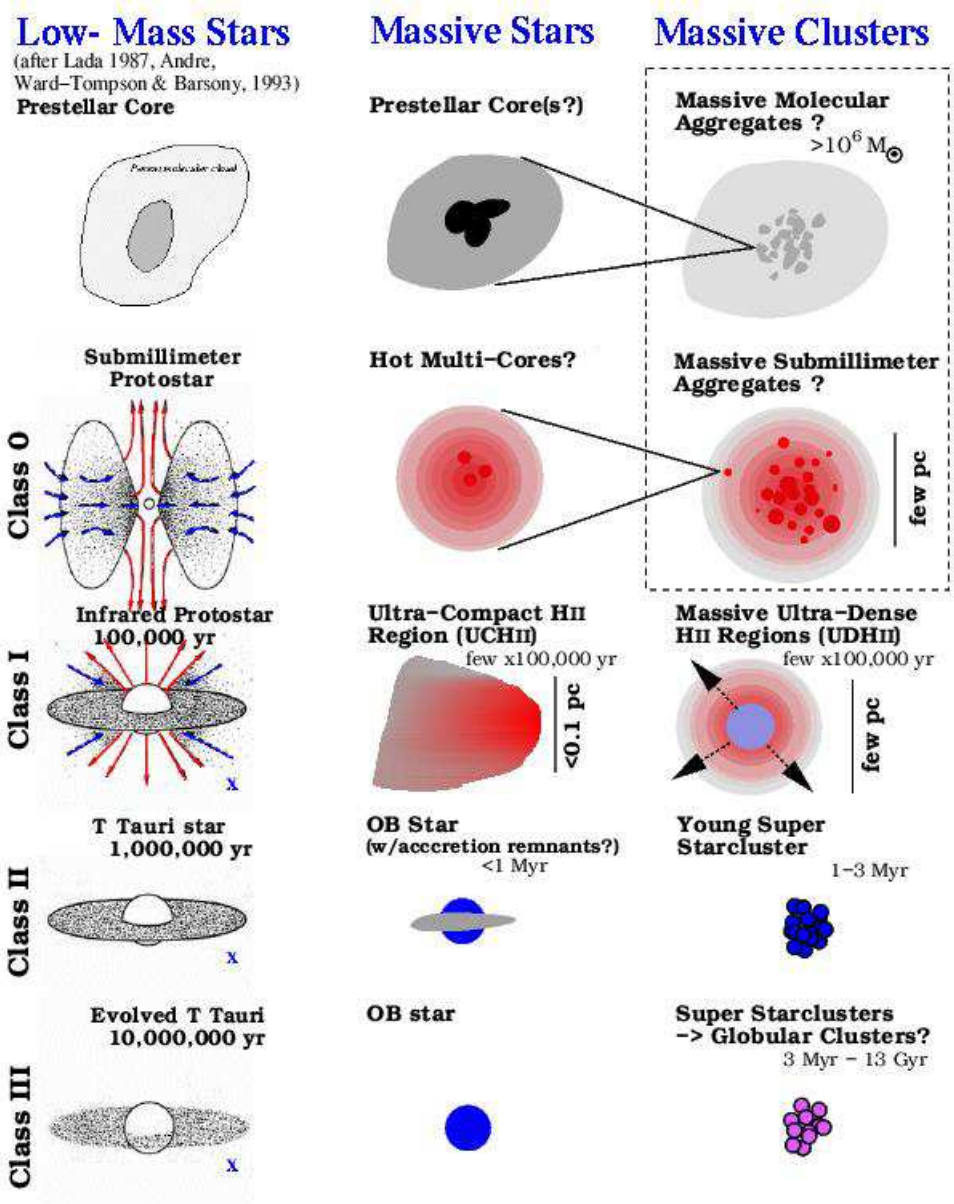

Figure 1.4: Schematic drawing of the different stages of low and high – mass star formation. The last column shows the evolution of a massive cluster and its fragmentation, which may be associated with massive star formation. The illustration was taken from http://physics.uwyo.edu/ chip/cluster_res.html.

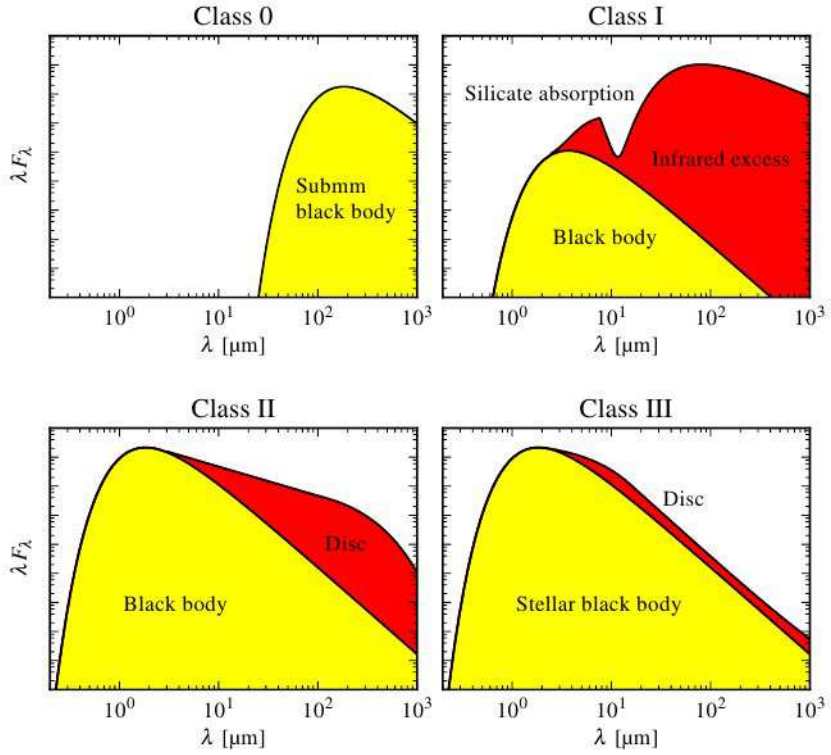

Figure 1.5: Spectral energy distributions (SEDs) of the different classes of low mass–protostars (André et al. 2000). The yellow areas correspond to the black–body radiation curves and the red areas represent the infrared excess compared to the black body.

According to the bolometric temperature definition we have a Class 0 object when T_{bol} <70 K, a Class I when 70 K<T_{bol}<650 K and Class II when 650 K<T_{bol}<2500 K (Enoch et al. 2009a). A Stage 0 object is characterised by an envelope mass M_{env} greater than the mass of the central heating source M_*, which can be translated to L_{bol} / L_{submm} < 200, under the assumption that L_{bol} relates to M_* and L_{submm} relates to M_{env} (André et al. 2000). At the same time a Class 0 object is characterised by an extended submillimeter continuum emission up to few 1000 au, which traces the envelope. In the transition between Class 0 and Class I the majority of the material is expected to have been accreted from the envelope into the central object and thus $M_* > M_{env}$ (M_{env}>0.1$M_\odot$). The Class II stage, is believed to correspond to the well known T–Tauri stage, during which the protostellar envelope has been completely dispersed (M_{env}<0.1$M_\odot$). In this stage the SED is dominated by the black body radiation of the pre–main sequence object and the disc. So L_{bol} / L_{submm} can be used as an indicator of the evolutionary stage of an object and it is expected to increase with time. Class II shows a much more compact structure of no bigger than a few 100 au.

The accretion rate reduces from $10^{-5}M_\odot$/yr to $<10^{-7}M_\odot$/yr and the outflow momentum from $\sim10^{-2}$ $M_\odot$ km s^{-1} to $\sim10^{-3}M_\odot$km s^{-1}, as we move to more evolved stages (Machida & Hosokawa 2013) while the lifespan of these objects increases by about an order of magnitude in each stage, from few tens of thousand years for a Class 0 object to

10^7 years for a Class III object, which is believed to be characterized by a debris disc.

High mass phases

Although in this thesis we do not study the evolutionary stages of high mass formation, a brief discussion is added for a more complete view and comparison with the low mass case.

Despite the difficulties to observe massive star–forming regions, observations have helped us to classify several phases of high–mass cores. It is very difficult to confirm that these phases are also evolutionary constraints, because of the fast scales that a massive star evolves, which complicates the differentiation between luminosity and evolution signatures.

The formation of a high mass star begins in high mass starless cores (HMSC) at densities $>10^6$ cm^{-3}, temperatures < 20 K and typical masses of few hundreds to thousands $M_\odot$. The Infrared Dark Clouds (IRDC), that are dark filaments with a bright infrared background, have been suggested to host cores of diferent evolutionary stages (Shipman et al. 2014). The high–mass protostellar object (HMPO) is the phase that possibly follows. This object does not appear at cm wavelengths that trace the ionized gas by free–free emission, it is lacking complex chemistry, and it is characterized by infall activity. After this, the complex organic molecules begin to enrich the spectrum of the object, as a result of the ice evaporation of the dust grains (Cesaroni 2005). An object that shows this chemistry is called a hot molecular core and it shows the transition to warmer phases of star forming regions as observed also in the low–mass case. Hot molecular cores may coexist with the phases that follow.

The fact that a a massive protostar can get hot enough to trigger hydrogen fusion and to enter the main sequence while still collapsing and accreting, is one of the main differences between low and high mass star formation. The accretion at this phase can be halted by the strong radiation pressure caused by the UV, and we have the appearance of the next evolutionary phase, the hypercompact/ultracompact HII regions with typical sizes between a few 100 to a few 1000 au. When the parental cloud is disrupted due to the expansion because of the radiation pressure, magnetic fields and turbulences and the stars can be observed in the optical and the near infrared windows.

1.2.3 Chemistry: hot cores and corinos

A third goal of this thesis is to understand the chemistry that characterizes low–mass protostellar envelopes and compare it with previously studied high–mass cases. Classical hot cores are located around young high–mass stars. These cores are characterized by high temperatures ($\geqslant$100 K) and high densities ($\geqslant 10^7$ cm^{-3}) and are of interest because of the complex organic molecules that they host (Herbst & van Dishoeck 2009). Similarly, a complex organic chemistry has been reported in the inner envelopes of low–mass

Class 0 protostars, the hot corinos. The observed chemical complexity is thought to be a result of evaporation from dust grains at temperatures of ∼100 K, which also indirect defines the physical size of the hot corino (R∼100 au). The formation of complex organic molecules on the icy grain surfaces is enhanced closer to the central object, and the evaporation occurs easily due to high temperatures, and these molecules enrich the gas. It is worth mentioning that although CH_3OH is by astronomical definition a complex organic molecule, its common presence in the ISM (Kang et al. 2013) separates it from a hot corino or core indicator. CH_3OH is easy to make (the simplest alcohol) and its formation is thought to take place almost entirely on grain surfaces of ISM where atoms meet and react, producing molecules. The mechanism for methanol production appears to be a sequence of surface reactions that begins with the abundant CO. H_2CO is an intermediary in this process. Methanol provides the major route to the formation of more complex less abundant organic molecules, which do not seem to build up in the same simple way (i.e. atom by atom) but rather by using pre-formed building blocks, such as methanol (e.g. section by section). CO freezing is suggested to be an important factor when it comes to the formation of CH3OH and of larger COMs (Ceccarelli 2008).

The chemistry that characterizes the ISM and star forming regions is a result of a variety of mechanisms. The formation of molecules cannot be described by a single process but overall we can explain the formation of relatively simple species by categorizing all the ongoing processes into two broader main mechanisms: gas phase chemical reactions (e.g. photodissociation, neutral–neutral, ion–molecule, dissociative recombination) and grain–surface chemical reactions that occur when gas phase species accrete, diffuse and react on the surfaces of small grains. The detailed description of the sub–processes is beyond the purpose of the current introduction; it can be found for instance in Tielens (2005, 2012).

Although we understand the gas–phase chemistry reasonably well, we only poorly understand the grain–surface chemistry and even less the gas–grain interaction. This lack of understanding becomes more important when attempting to understand in detail the chemistry of special environments such as hot cores, where gas–grain interaction leads to the evaporation of the ice mantles and the enrichment of the gas with grain–surface products This fact increases the uncertainties of our models for complex molecules (e.g. CH_3OH) which can reach orders of magnitude..

1.3 Long wavelength observations

Molecular clouds are too cold to emit visible light, and are usually studied at infrared and radio wavelengths. The greatest challenge in infrared astronomy is that almost all the radiation gets absorbed by the water vapor in the Earth's atmosphere. Even the highest observatories have only a limited access when it comes to mid– and far–infrared and (sub-)mm–wave radiation (5 μm – 3 mm, Figure 1.6). From this fact one can easily understand the necessity of observatories at really high altitudes and dry environments, but also the

importance of stratospheric and space missions. This thesis uses a variety of instruments in this field ranging from single–dish ground–based observatories (i.e. JCMT, IRAM) to interferometer (CARMA) and up to stratosphere (SOFIA) and space (Herschel).

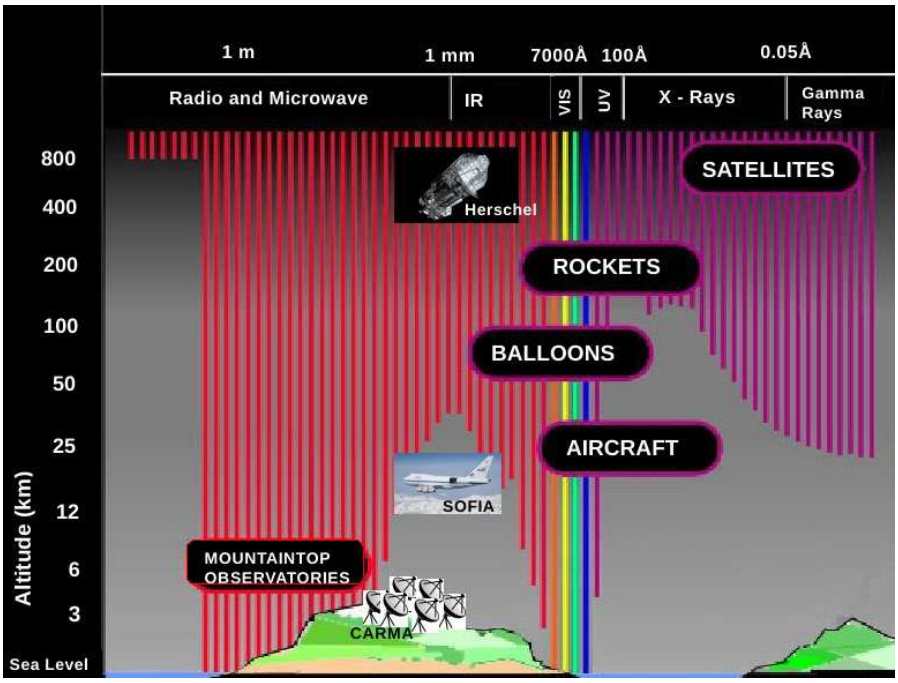

Figure 1.6: Atmospheric transparency for the different wavelengths of the electromagnetic spectrum. Molecular clouds, environments of star formation, are usually studied at infrared and radio wavelengths.

Spectroscopy plays a crucial role in our understanding since it is the main tool yielding information on the physical and chemical properties of these regions. By studying spectra we gain information about the temperature, density, collapse rate, velocity structure, the chemical abundances and chemical distribution of the protostellar envelopes and their surrounding environment.

Not only molecules, but also dust is essential in star–forming regions. At temperatures of 10–100 K, dust emits strongly at (sub–)millimeter wavelengths as continuum emission. In particular, by knowing the total flux density of this emission, the Planck function for given dust temperature, the opacity and the distance of the emitting area, we can estimate the total dust mass of this area. We can then find the mass of the gas after the assumption that gas–to–dust is 100.

1.3.1 Ground based observations

- The JCMT Spectral Legacy Survey (SLS)

The JCMT Spectral Legacy Survey (SLS; Plume et al. 2007) is one of seven big surveys that all together make up the more general JCMT Legacy Surveys (JLS) programme. The aim of JLS is to study our Galaxy and the Universe at sub-millimeter wavelengths using the capabilities of the James Clerk Maxwell telescope on the summit of Mauna Kea in Hawaii. The SLS focuses on star formation. It uses the unique spectral imaging capabilities of the 16–element Heterodyne Array Receiver Programme B (HARP–B) and the Auto–Correlation Spectral Imaging System (ACSIS) to study the molecular inventory and the physical and chemical structure of several objects, including NGC 1333 IRAS 4 region, which contains three low mass protostellar systems, and is a target of interest in this thesis (Chapters 4 and 5). NGC 1333 IRAS 4 was mainly chosen because it is one of the first and youngest proto-binaries ever detected (IRAS 4A and IRAS 4B), while previous studies have shown a binary nature of these individual systems and interesting chemical differences between them. The SLS produces for the first time a spectral imaging survey that covers the wavelengths of the entire window from 330 GHz to 375 GHz, providing the spatial ($2' \times 2'$ maps) and velocity distribution of all the covered detected molecules. This allows the examination of both sources in more detail and over a more extended area than was possible before.

- IRAM – Institut de Radioastronomie Millimétrique

The IRAM 30m telescope is one of the most large and sensitive millimeter telescopes, and it is located at an altitude of 2850 m on Pico Veleta in Sierra Nevada, Spain. It provides mapping capabilities and high resolution spectroscopy at 0.9, 1, 2 and 3 mm wavelengths. It has made a great contribution on studying the chemistry and the physical processes that take place during star formation within the molecular clouds of the Milky Way and beyond. This thesis uses the mapping capabilities ($4' \times 4'$ maps) from this telescope towards the S 140 star forming region, at 1 and 3 mm (Chapters 2 and 3).

- CARMA – The Combined Array for Research in Millimeter-wave Astronomy

CARMA (2006–2015) was one of the most powerful millimeter arrays in the world providing great wide–field heterogeneous imaging capabilities and sub-arcsecond angular resolution which can be as high as $0.15''$. It consists of up to 23 antennas that can be used in combination in order to provide maps at millimeter wavelengths, and more specifically it provides a broad frequency coverage, covering the atmospheric windows 27–35 GHz (1 cm), 85–116 GHz (3 mm) and 215–270 GHz (1 mm). In this thesis we use both continuum and molecular line observations taken with the array of 15 antennas at 1 mm. It is the only interferometer used in this thesis and the data cover only the NGC 1333 IRAS 4C dense core (Chapter 4).

1.3.2 Stratosphere based observations – SOFIA

The Stratospheric Observatory for Infrared Astronomy (SOFIA) is a modified Boeing 747SP aircraft that carries a reflecting telescope of 2.5 m. It is the largest airborne observatory in the world. The infrared light that SOFIA is capable to observe cannot reach even the largest ground–based telescopes that are located at the highest altitudes mostly due to to the water vapors on Earth's atmosphere that absorbs these wavelengths. In this thesis we use observations from the German REceiver for Astronomy at Terahertz Frequencies (GREAT) which is a dual channel heterodyne instrument that provides spectra of high resolution (Chapter 3) and continuum images from the Faint Object infraRed CAmera (FORCAST) which is a dual–channel mid–infrared camera sensitive from 5–40 μm (Chapter 2). This dataset was targeting the S 140 photon-dominated region with as main goal the study of the thermal balance in the region and the influence of internal and external radiation under a clumpy environment.

1.3.3 Space based observations – Herschel

The Herschel Space Observatory (2009–2013), had a mirror of 3.5–m diameter making it the largest space telescope ever launched. In addition Herschel was the only space observatory that covered electromagnetic radiation from the far–infrared to the sub–millimeter. Herschel had three instruments on board: the Heterodyne Instrument for the Far Infrared (HIFI), the Photodetecting Array Camera and Spectrometer (PACS) and the Spectral and Photometric Imaging Receiver (SPIRE).

In this thesis we use data from HIFI and PACS towards both regions of interest (Chapters 2, 3 and 5). HIFI is the only instrument that permits high spectral and spatial resolution along with higher sensitivity over the 500–2000 GHz frequency range, which is hardly observable from the ground. Herschel gives us the opportunity for an extended study that was not possible before due to these limitations and thus provides an important unbiased survey. In this frequency range, there are several molecular and atomic transitions that are crucial for understanding the energy balance, chemical composition, and physical structure of star forming regions. In addition we use the imaging capabilities of PACS, an imaging camera and low–resolution spectrometer which covered the range from $\sim 57 - 210$ μm.

The HIFI datasets used in this thesis are part of the "Warm And Dense Interstellar medium" – WADI for S 140 (Ossenkopf et al. 2011) and the "Chemical HErschel Surveys of Star forming regions" – CHESS (Ceccarelli et al. 2010) key programmes of Herschel.

1.4 Analysis–Methods

As mentioned before, this thesis is dealing with both spectral line and continuum datasets. For the spectral analysis of a wide range of wavelengths, one has to identify spectral lines. All the identifications presented in this thesis are based on the use of databases, more precisely the Cologne Database for Molecular Spectroscopy – CDMS (Müller et al. 2001), and the Jet Propulsion Laboratory – JPL (Pickett et al. 1998), that are combined in a common interface[1] for molecular line identification.

After the correct identification, the lines can be investigated and measured for scientific analysis / interpretation. The usual shape of a line (profile) is a result of a Gaussian component due to Doppler broadening and turbulence and a Lorentzian component due to the uncertainty of the energy of the excited state (uncertainty principle). The last one is also known as natural broadening. The Lorentzian component can also be a result of collisional/pressure broadening which reduces the lifetime of the upper state, Δt, and increases the uncertainty ΔE. At the studied wavelengths the line profile is dominated by the Gaussian component. A first look at the shape of the line can already give us information regarding the environment from where the line originates. For example, outflow activity causes a broad profile that can only be fitted by multiple Gaussians, compared to a line that has its origin to quiescent gas and thus show a single narrow regular Gaussian profile. Further signatures such as infall and expansion, can also be traced by absorption features. Fitting the lines with one or multiple gaussians one can derive useful information such as the central velocity of the emitting gas, and thus the kinematics of the region, the width of the lines and thus trace rotation or outflows and the integrated intensity of the lines $W = \int T_{mb} dV$ expressed in the unit K kms^{-1}. The integrated intensities of the lines are used for more detailed modeling in order to measure physical parameters such as temperatures and densities of the regions, and also to infer their chemical composition.

In order to understand the physical conditions that the molecular line or dust continuum emission traces, we need to compare the observed emission with the one that the physical models produce. These models range from simple population level equations using local thermodynamic equilibrium (LTE) to more complex radiative transfer models that take into account non–LTE effects and chemical abundances, which is probably closer to reality. In addition the chemistry of the regions can be better studied by deriving time dependent chemical abundance profiles using chemical codes.

In this thesis we use a variety of models in order to achieve a better understanding on the physics and chemistry that characterize our regions of interest, and thus on star formation. We therefore use a) population diagrams for a rough excitation analysis of the envelope and outflow of a protostellar envelope, b) Radex (van der Tak et al. 2007a) for an estimation of kinetic temperatures, densities and column densities towards both our regions using ratios of CO and H_2CO, c) RATRAN (Hogerheijde & van der Tak 2000) for a more sophisticated radiative transfer model that takes into account the physical structure of the sources using temperature and density gradients, d) a PDR code based

[1] http://www.splatalogue.net/

on Kaufman et al. (1999) which is suitable for studying the thermal balance towards the S 140 PDR region, taking into account the radiation field and the geometry of the source and e) the ALCHEMIC (Semenov et al. 2010) code as a more sophisticated way to derive the several time dependent chemical abundances towards the low mass protostellar envelope and compare them with the observed abundances derived with RATRAN. The exact usage of codes in the upcoming chapters and the scientific goals to be achieved are described below.

1.4.1 Local thermodynamic equilibrium – LTE modeling

In astronomy, we often have to work with various temperatures such as effective temperature, color temperature, excitation temperature, ionization temperature and kinetic temperature, all described by different equations. The beauty of a system in thermodynamic equilibrium is that it is possible in all these equations to use a single temperature T.

The entire concept of thermodynamic equilibrium is based on two simple but crucial hypotheses: isotropy applies, which means that the physical properties (e.g. density, temperature) are the same independent of the direction, and homogeneity, which means that the properties remain the same at all positions. Such ideal conditions never apply 100% to real astronomical objects. In particular, our objects of interest, are characterized by much higher temperatures in their center than their outer parts. To deal with such situations, astronomers often consider a system in local thermodynamical equilibrium (LTE), which applies as soon as collisions dominate the de-excitation process, and all the transitions are populated by a single excitation temperature $T_{\rm ex}$.

One of the temperatures used in this thesis is the kinetic temperature T_{kin} which describes the velocities υ of the particles in a system, following the Maxwell–Boltzmann distribution:

$$f(\upsilon) = 4\pi\left(\frac{m}{2\pi k T_{kin}}\right)^{\frac{3}{2}} \upsilon^2 e^{-\frac{m\upsilon^2}{2kT_{kin}}} \tag{1.1}$$

where m is the mean mass of the particles, T_{kin} the kinetic temperature of the gas, υ the velocity of the particles in the system and k the boltzmann constant.

In the case of a simple system with only two energy levels E_u and E_k, the ratio between the population of these levels can be described by the Boltzmann factor:

$$\frac{n_u}{n_k} = \frac{g_u}{g_k} e^{-\frac{h\nu_0}{kT_{ex}}} \tag{1.2}$$

where T_{ex} is the excitation temperature, g_u and g_k are the statistical weights of the levels and ν_0 is the frequency of this single transition, being equal to $(E_u - E_k)/h$ and h the Planck's constant.

In thermal equilibrium, the radiation field of a body can be described by the radiation temperature T_{rad}. Its distribution is described by the black body Planck function per unit frequency v:

$$B_v = \frac{2hv^3}{c^2} \frac{1}{e^{\frac{hv}{kT_{rad}}} - 1} \tag{1.3}$$

Population diagrams

A widely used method to estimate the rotational temperature of a system is the population diagram. The basic idea of this method is that the system is in LTE, which means that all molecules are thermally excited and thus the rotational excitation follows the Boltzmann distribution and the local temperature can be measured by the optically thin emission. With simple words: $T_{ex} = T_{kin} = T_{rad} = T$ of the system. This approach is valid as soon as the density of a region is characterized by densities above the critical density of the molecular transitions, which is defined as the ratio between the radiative processes of excitation (Einstein coefficients) over the excitation of molecules caused by collisions. The reader should note that LTE is not universal for all molecules under certain conditions but it depends on the molecule and the line transition since the critical densities vary for each molecule and each transition. Thus, for example from the same gas, low-J CO lines may be in LTE, but HCN lines and high-J CO lines may not. Every molecule will be in LTE under certain conditions. As an example, CO 2-1 will be in LTE for densities $n_{H_2} > 2\times10^4$ cm^{-3} while HCO^+ 2-1 will be in LTE for densities $n_{H_2} > \times10^6$ cm^{-3}.

The temperature of the system when in LTE can then be determined by:

$$\frac{N_u}{g_u} = x\frac{\int T_{mb}dV}{v\mu^2 S} = \frac{N_T}{Q(T_{rot})} e^{-\frac{E_u}{T_{rot}}} \tag{1.4}$$

where $x = 8.591\times10^{37}$ $8\pi k/hc^3$, N_u the column density of the upper energy level (cm^{-2}), g_u the degeneracy of the upper energy level, T_{mb} the main beam temperature (K), dV the velocity range (kms^{-1}), v the frequency (Hz), μ the dipole moment (D), S the line strength, N_T the total column density (cm^{-2}), T_{rot} the rotational temperature (K), Q the partition function (can be found in CDMS for a given rotational temperature) and E_u the upper energy level.

This method can work well for some molecules in dense regions where LTE is expected. It gives an idea of the average excitation temperature, but fails to deal with temperature gradients. Furthermore, it can only be used for optically thin lines. This means that the method does not work for molecules with high column densities, and thus the rare isotopologues are preferred.

Overall, the following factors can result in temperature and column density estimations that differ significantly from their real values: non–LTE excitation (sub-thermalization), high optical depths and beam effects. By beam effects we mean the divergence from homogeneous conditions inside the beam, i.e. excitation gradients within the beam, and the beam dilution as a result of different angular resolutions among the lines used for the analysis. Goldsmith & Langer (1999) describe these effects, and propose to use the modified equation:

$$ln\frac{N_u}{g_u} = ln\frac{N_{T,thin}}{Q(T_{rot})} - \frac{E_u}{kT_{ex}} - ln(C_\tau) + ln(f) \tag{1.5}$$

where C_τ is the optical depth correction factor, and f the beam dilution which is defined as the size of the telescope beam over the size of the emitted region.

However, star forming regions are characterized by temperature and density gradients and the several molecular transitions can arise from different layers and thus trace different excitation conditions. For more accurate modeling one has to take into account non–LTE effects and temperature and density gradients.

1.4.2 Non–LTE modeling

The LTE approach does not work if any of the following play a role: optical depth effects, sub–thermal and supra–thermal excitation ($n < n_{cr}$ i.e. $T_{ex} \neq T_{kin}$), radiative pumping and population inversion (i.e. maser emission) and formation pumping. The later is caused by exoergic chemical reactions that cause $T_{ex} \gg T_{kin}$ and a molecule is formed in an already higher excitation level. The last two effects only occur in specific situation and require the use of specialized programs.

Here we describe the radiative transfer non–LTE codes used in this work which can calculate efficiently model grids that can be used for the comparison with observational data. The setups of each code vary in a way that one can assume model geometry, physical and chemical structure and choose the number and the nature of the free parameters.

RADEX

The RADEX code (van der Tak et al. 2007a) uses the basic equations of radiative transfer and it can be used to analyze molecular line observations. By default it assumes an isothermal homogeneous spherical cloud of gas, with the possibility of expansion motions if needed, and it takes into account both radiative and collisional excitation and optical depth effects. In most of the cases the velocity–integrated line intensity is modeled, after the assumption that the excitation is independent of velocity. The temperature T_{kin}, the density n_{H_2}, the molecular column density N are input parameters, and in the

simplest case the first two parameters are known (i.e. from previous observations). In addition the observed line width and the radiation field (e.g. CMB) are input parameters. Collisions with H and electrons are not taken into account in protostellar envelopes where both components are less abundant but they may play a role in PDRs (e.g. Nagy et al. 2013).

The program can be used in two ways: one can compare modeled line intensities with the observed ones or one can compare the observed intensity ratios of lines of the same molecule, for given conditions with the observed and determine temperatures and densities, which depends on the sensitivity for specific ratios to temperatures or densities. The ratios between main and rarer isotopologues can be used to estimate molecular column densities.

RADEX does not take geometry effects into account. Not knowing the structure of the source makes the correction for beam dilution crucial, when the source is not resolved. The easiest and more consistent way to deal with that is by modeling the line ratios instead of individual fluxes under the assumption that the beam dilution is similar for both lines, which is not always the case since the resolution often is not constant but it changes with frequency Using lines of similar resolution and convolving mapping observations when available to the same resolution is the recommended approach.

In this work, RADEX is used as a tool in constructing maps of kinetic temperature, column and volume density across the regions, by using suitable species. This was done by performing a χ^2 minimization for a set of parameters. For the model input we used the molecular data from the Leiden Atomic and Molecular Database (LAMDA) (Schöier et al. 2005) which provides the atomic and molecular data needed for the excitation calculation, and the most recent collisional rate coefficients (e.g. CO; Yang et al. 2010).

RATRAN

RATRAN (Hogerheijde & van der Tak 2000) is a Monte Carlo radiative transfer code for 1D and 2D spherical or cylindrical symmetric structures, which takes the radiative transfer modeling as described above a step further, by taking into account the detailed temperature and density structure of the emitting area. If the physical model that defines the temperature and density gradients is known (i.e. by dust continuum models of a region), then RATRAN defines shells of gas that follow this structure producing more accurate solutions. The produced line profiles should be convolved according to the beam size of the used telescope in order to be able to direct compare the results with the observations. The most common assumption in RATRAN is thermal equilibrium between dust and gas ($T_{gas} = T_{dust}$) which is valid for high volume densities ($>10^5 cm^{-3}$) which applies to both regions of interest. In any case, the user has the freedom to use different temperature gradients for dust compared to gas, if there is an indication of the decoupling of the two as we found in S 140 in this thesis (Chapter 2).

In this thesis we use RATRAN in two situations: we import the best fitting dust model

derived using continuum observations in RATRAN, and compare the resulting modeled lines with the observations (Chapter 2) and we compare the empirical abundance profiles with those resulted from chemical models (Chapter 5).

PDR codes

As we mentioned in Sec. 1.1.2 most of the ISM is actually in PDRs. This fact makes the development of PDR models very important when it comes to the interpretation of ISM observations in multiple environments. Two of our chapters (2 and 3) study the S 140 PDR and thus the use of a PDR code for the better understanding of the observations is crucial.

We use the PDR model based on Kaufman et al. (1999). As the majority of PDR codes, it solves the coupled equations of thermal balance (heating and cooling), chemical equilibrium, and radiative transfer in spherical symmetry in PDRs. Having to deal with all these processes simultaneously, it takes into account the grain photoelectric heating rates, the chemical rate coefficients and atomic and molecular data.

This code assumes gas–phase elemental abundances and OH5 grain properties (MRN with thin ice mantles) taken by Ossenkopf & Henning (1994a), which was found to well represent star–forming regions (Evans et al. 2001). Furthermore is uses a constant value for the volume density throughout the PDR, and the intensity of the FUV radiation field at the surface of the PDR G_0 (proportional to the standard ISRF in units of Draine field). These are the input parameters together with the microturbulent velocity dispersion of the gas. The abundances of polycyclic aromatic hydrocarbons (PAHs) are also included (4×10^{-7}), since dominate on the the grain–photoelectric heating. The grain photoelectric heating rate was derived including a size distribution of particles: from large grains of 0.25 μm to small PAHs of 5 Å.

In this thesis we use a simple model in order to treat the PDRs in S 140 (Chapter 3) as a face–on configuration taking the optical depths of the lines into account simulated by Kaufman et al. (1999). In the model we apply only two free input parameters: the volume density and the radiation field, the strength of the UV radiation field being the most crucial, and compute the line and continuum intensities. We derive the source parameters by comparing the [C II] line intensity, the [O I]/[C II] intensity ratio, and the ([O I]+[C II])/TIR ratio from model predictions (Figs. 3-6 from Kaufman et al. 1999) with the observed values. The inclination angle can also be used as an additional free parameter.

1.4.3 Modeling the dust emission – DUSTY

In order to model the continuum emission and construct the physical structure of the main heating source IRS in S 140 region and derive its temperature and density gradients we use the DUSTY code. The radiation we receive from star forming regions, is not the

original radiation from the embedded central object, but the one processed by dust. The dust absorbs, scatters and re–emits the original radiation from the embedded central star providing the spectral energy distribution which we can model. The radiative transfer in a steady state and its simplest form is given by:

$$\frac{dI_\lambda}{d\ell} = \kappa_\lambda(S_\lambda - I_\lambda) \tag{1.6}$$

where κ_λ is the total (absorption and scattering) extinction coefficient at λ, $\kappa_\lambda d\ell$ is the optical depth $d\tau_\lambda$, S_λ is the source function and I_λ the intensity.

The DUSTY code (Ivezic et al. 1997) solves the radiation transport equation in the dusty circumstellar environments that surround stars and is able to do so for both the optically thick and the optically thin cases. The solution method is based on a self-consistent equation for the radiative energy density. It includes dust scattering, emission and absorption, and it is exact to the numerical accuracy that was specified. For all the formulas used the reader should go to the original paper.

There are many input parameters in DUSTY. The properties of the radiation source and the dusty region need to be implemented, and as a result the code gives the dust temperature distribution and the radiation field that characterizes this region. In fact the input consists of the physical parameters, numerical accuracy parameters and flags for additional output files. The input physical parameters are the characteristics of the external radiation (i.e. spectral shape), dust grain properties, and the density distribution of the envelope. The optical properties (i.e. dust absorption, scattering cross–sections) depend on the chemical composition and the size distribution of the grains, and for the most common types of astronomical dust (Ossenkopf & Henning 1994a), DUSTY has them already built in and they are used to produce optical depths. Another important input parameter is the dust temperature on the shell inner boundary.

For the given set of parameters, DUSTY generates up to 1000 models with different optical depths. For each optical depth, the output file contains the bolometric flux at the inner radius, the inner radius of dust temperature T_{in}, which scales with luminosity, the r_{in}/r_c, where r_c the radius of the central source, the angular size in arcsec of the shell inner diameter and the dust temperature at the outer shell of the envelope. In the end one can compare the best fit modeled SED with the observations and get a full list of the properties that describe the region.

In this thesis the density and temperature gradients as derived with DUSTY are used for further modeling of the lines using RATRAN.

1.4.4 Chemical models

Molecules play an important role in our understanding of the star–formation process. Trying to understand the molecular mechanisms is crucial in our further understanding of the evolutionary phases, the astrochemical complexity and the overal physical conditions that characterize such regions. In order to calculate the abundances of the molecules in

the current phase of a region, one has to solve a number of equations implementing the initial conditions and abundances.

We are interested in deriving the time dependent chemical abundances of the observed species towards a low mass protostellar envelope, an environment with a weaker UV radiation compared to high mass protostellar environments (PDRs) and which is mostly the result of accretion and shocks. The chemical models used in this thesis are based on the time dependent gas–grain chemistry ALCHEMIC code (Semenov et al. 2010). Gas–phase processes were previously thought to be the key mechanisms for formation of more complex organic molecules in star forming regions (van Dishoeck & Blake 1998). These mechanisms, however, have been considered to be inefficient and the grain–surface chemistry has been proposed instead (Garrod 2008). The gas–grain chemistry involves chemical processes such as the loss of atoms and molecules from the gas to the grains, the catalytic reactions on the surfaces of the dust grains and the enrichment of the gas through the return of the surface species to the gas–phase.

In these models one sets the chemistry network. In this thesis we used a chemical network which is based on the gas-phase osu032008 ratefile [2] (Albertsson et al. 2013) which includes gas–grain interactions and a set of surface reactions for the H-, O-, C-, S-, and N-bearing molecules. The chemical processes in this code include both gas phase, gas–grain, and surface reactions (as described in Sec. 1.2.3). The surface reaction rates are calculated assuming no H/H_2 tunneling through potential walls of the surface sites.

The input parameters of these models include: the physical structure, i.e. temperature and density profiles as derived using continuum observations, the cosmic ray ionization rate, ζ_{CR} (5×10^{-17}s^{-1} for NGC 1333 IRAS 4A), the dust radius and density, dust–to–gas mass ratio (0.01) and the diffusion / desorption ratio for surface species (0.77). This conservative value was used until recently and it was adopted from Ruffle & Herbst (2000). An exact value is not that well known but seems closer to 0.3-0.5, based on experimental results. If a lower value had been used, more complex organics species would have been formed. These models are time dependent, thus the age of the object of interest which is also important could be derived by comparing the modeled profiles for a range of timescales, which can be from 1 year up to 10^9 years. We need to clarify that we can derive the best-fit age of our object in the framework of the model that we use. If in reality conditions are quite different or our chemical network misses some key reactions, the best-fit age value can be quite different from reality. A rigorous way to do such modeling would require running numerous models with varying T, ρ, CR ionization rate, and reaction rates. In this thesis we use a more narrow range (10^3–10^6 years) based on previous estimates of the age of our object (10^4–10^5 years).

In order to derive the abundance profiles from the species of interest one has to set the initial abundances. The model uses a set of 12 elemental abundances from Wakelam & Herbst (2008). These species include H, He, N, O, C, S, Si, Na, Mg, Fe, P and Cl. All elements are assumed to be initially atomic and ionized, except from hydrogen which is

[2] http://web.archive.org/web/20131408091500/http://www.physics.ohio-state.edu/ eric/researchfiles/osu032008

assumed to be entirely molecular, and He, N and O that are only assumed to be neutral and all heavier elements are depleted from the gas phase, and all grains are neutral. The result of this process are abundance profiles from the species of interest. This means that we get the abundance of species over the radius adopted for the physical models for a range of timescales.

In this thesis, we calculate the abundance profiles for several species and compare them with empirical RATRAN models, in our attempt to a) understand the chemical processes that take place in one of our sources (NGC 1333 IRAS 4A), b) constrain its age and c) compare this low mass case with a high mass case from the literature (AFGL 2591).

1.5 This thesis

Our goal for the present low mass to high mass star formation thesis is to cover different luminosities and different evolutionary phases of young stars and understand the physical and chemical processes that take place in these regions. The sources being studied in this thesis, the questions and the context of the scientific chapters are described below.

1.5.1 Targets

For the selection of our sources it was crucial to consider regions that host both high-mass and low-mass protostars. The Class 0 sources are believed to represent the first stages of the collapse that take place in low mass star formation for some years already (Mardones et al. 1997). Simultaneously with the infall, violent outflow winds/jets eject matter outwards. NGC 1333 provide a perfect laboratory for low mass star formation, while S140 is used in this thesis for the study of high mass stars and PDRs.

a) NGC 1333

NGC 1333 is one of the most nearby (D=235 pc; Hirota et al. 2008) and young ($<$ 1 My; Gutermuth et al. 2008) star forming regions. It is one of the best studied regions and it hosts low to intermediate mass stars. It is a part of the Perseus OB2 molecular cloud complex and it contains a large number of young stellar objects (YSOs), which are stars in the earliest stages of development. It hosts about 50 YSOs and 36 Herbig–Haro (HH) objects. The Herbig–Haro objects are regions that show nebulosity due to the jets produced by newly born stars and thus they are associated with star formation. Newly born stars are often only visible at infrared wavelengths, being heavily obscured by dust. Far infrared wavelength observations have revealed the IRAS 4 region, which hosts a number of highly embedded infrared sources that are connected to young low mass stellar objects. We are particularly interested in IRAS 4A, IRAS 4B and IRAS 4C. IRAS 4A and IRAS 4B appear as the two brightest continuum objects and are classified as Class 0 objects while the nature of IRAS 4C is under debate.

b) S 140

S 140 (Figure 1.7) is an HII region that lies at the south–west edge of the molecular cloud L1204 at a distance of 746 pc (Hirota et al. 2008). This region provides strong evidence of several phenomena associated with star formation of various masses. More specifically, outflows and strong UV radiation are highly connected to the process of high–mass star formation. S 140 is an ideal environment for the study of the effects of radiation from both internal and external heating sources that create photon-dominated regions (PDRs). On one hand we have a BOV star (HD 211880) around 1.8 pc away from the cloud that illuminates the edge of L1204 creating a PDR region firstly seen by Crampton & Fisher (1974). On the other hand we have several high-mass star infrared sources with IRS1-3 the most luminous.

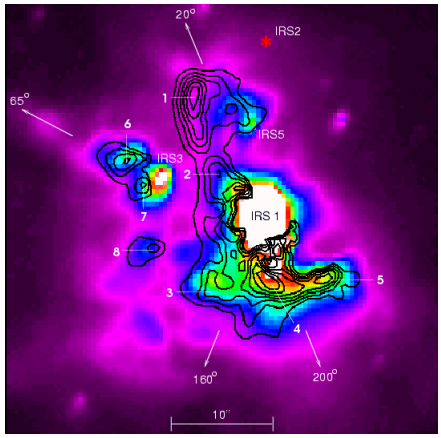

Figure 1.7: 2.12 μm H_2 map of the S140 IRS region ($\sim 45'' \times 45''$): The positions of the deeply embedded infrared sources IRAS 1 (central), IRS 2 and IRAS 3 are well shown (Preibisch & Smith 2002).

Two bi–polar outflows can be found in the S 140 cloud (Preibisch & Smith 2002). One is traced by observations of shock like features and H_2 knots, which provide strong evidence of hot, shocked gas, lined up northeast of IRS 1 over several degrees. The other, which is perpendicular to the first, has been observed in CO.

1.5.2 Specific questions and components of this thesis

In this thesis I study the influence of forming stars on their surrounding matter (PDRs; Chapter 2, 3), and the physical and chemical structure of protostellar environments, and address the potential chemical differences among low and high mass objects (Chapter 5). I also aim to trace the evolutionary status of dense cores (Chapter 4).

Questions

The specific questions that we are addressing in this thesis are:

- What is the thermal balance, the chemical and dynamical structure in PDRs and what is the impact of UV radiation and clumpiness in such environments ? (Chapter 2, 3)
- How can we constrain the evolutionary state of dense cores? (Chapter 4)
- What is the physical and chemical structure of low mass protostars? How does their chemical structure compare to the high mass case? (Chapter 5)
- How do outflows influence the chemistry of the protostellar surroundings? (Chapter 5)

Components of this thesis

In **Chapter 2** of this thesis we study the thermal equilibrium between dust and gas in a sub–area (IRS 1–3, Ionization Front) of the photon-dominated S 140 region which is characterized by high densities ($\geqslant 10^5$ cm^{-3}) **(1st question in the list above)**. For this purpose we derive the dust and gas temperatures independently. We model continuum observations from Herschel PACS combined with SOFIA/FORCAST images and SCUBA data, using simple greybody fits and the more advanced DUSTY radiative transfer code. In addition we derive the gas temperature by modeling CO transitions as observed with the IRAM–30m over a $4'$ field and HIFI single points using RADEX. Moreover we use the density and temperature gradients as derived with DUSTY, as input to the more advanced radiative transfer model RATRAN. In contrast to expectation, we find that the gas is systematically warmer than the dust by at least $\sim$5–15 K despite the high gas density, and we conclude that this is a result of a deep UV penetration from the embedded sources in a clumpy medium and/or oblique shocks.

In **Chapter 3** we try to understand the thermal balance **(1st question)** by studying the gas heating and cooling in the S 140 star–forming region. For this purpose we use maps of the main cooling fine-structure lines of [O I] (63 μm) and [C II] (158 μm) and the rotational transitions of CO 13–12 and 16–15 observed with SOFIA/GREAT combined with IRAM–30m and Herschel observations that trace the energy input and the density and temperature structure of the source. We perform radiative transfer computations for all observed transitions and we assess the total cooling budget and measure the gas heating efficiency with the help of the far–infrared continuum. Striking is the fact that the main emission of fine–structure lines in S 140 stems from a $8.3''$ region close to the infrared source IRS 2 that is not prominent at any other wavelength, while the main heating source IRS 1 lacks associated emission that we cannot explain. We measure line-to-continuum cooling ratios $< 10^{-4}$. These values are lower than in any other Galactic

source, and are actually matching the far–IR line deficit seen in Ultraluminous infrared galaxies (ULIRGs [3]). This deficit is still difficult to explain, a fact that makes S 140 a great template that may lead to a future model.

In **Chapter 4** we investigate the evolutionary stage **(2nd question)** of three low mass objects that are previously classified as Class 0 based on their bolometric temperature. We directly compare the objects using molecular line observations from the JCMT Spectral Legacy Survey and line and dust continuum observations from CARMA. We set observational constraints others than the T_{bol}. More precisely we report differences between the three sources in four aspects: a) the kinetic temperature as probed using the H_2CO lines are much lower towards IRAS 4C than the other two sources, b) the line profiles of the detected species show strong outflow activity towards IRAS 4A and IRAS 4B but not towards IRAS 4C, c) the HCN/HNC abundance ratio is < 1 towards IRAS 4C, which confirms the cold nature of the source, d) the degree of CO depletion and the deuteration are the lowest towards the warmest of the sources, IRAS 4B. Based on our findings, IRAS 4C seems to be in a different evolutionary state than the IRAS 4A and IRAS 4B sources, but our results are not fully consistent with a younger or older object, with the major issues being the absence of outflow activity and the cold nature of IRAS 4C which could point towards a first hydrostatic core. A more detailed physical model of IRAS 4C is one of our future plans.

Finally the main goal in **Chapter 5** is to study the chemical structure of the low–mass Class 0 YSO NGC 1333 IRAS 4A and study the richness of the observed molecular species of the envelope and try to distinguish between a hot corino and a shock chemistry **(3rd and 4th question)**. We also aim to compare our results with a high mass case. For this study we use observations obtained with HIFI and JCMT and we use the Monte Carlo radiative transfer code RATRAN to create empirical abundance profiles and compare them with the ones derived from the time dependent chemical models (ALCHEMIC). In addition we try to constrain the age of this object by using the best fit results between the chemical and empirical models. We find that the outflow cavities are important for the chemistry of the low-mass protostellar environment, unlike high-mass case where hot cores dominate. In addition, H_2D^+ shows a very different spatial distribution compared to other ions and deuterated species and it probably arises from a colder foreground layer of gas. A more detailed 2D–3D chemical model, including a disk structure and outflow cavity is in our future plans. Investigating the spatial distribution of deuterated species in a larger sample of sources known to contain outflows is also a topic of interest for the future.

[3] Lower than expected [CII]-to-FIR ratios were first reported towards galaxies with high star formation activity (high [60 μm] / [100 μm]) using ISO observations (Malhotra et al. 1997)